



# Polymorphism in high-temperature GeS<sub>2</sub>: identification and characterization of two distinct polymorphs

Masaru Nakamura<sup>1,\*</sup> and Yoshitaka Matsushita<sup>1</sup>

<sup>1</sup> National Institute of Materials Science (NIMS), 1-1 Namiki, Tsukuba, Ibaraki 305044, Japan

**Received:** 24 December 2025

**Accepted:** 5 May 2026

**Published online:**  
17 May 2026

© The Author(s), 2026

## ABSTRACT

High-temperature (HT-) GeS<sub>2</sub>, a promising layered 2D material, has long been considered a single crystallographic phase. Here, we report the definitive identification of two distinct polymorphs, designated Polymorph A and B. A comprehensive structural and optical characterization revealed their contrasting properties. X-ray diffraction analysis showed that while both polymorphs possess a layered structure, their fundamental stacking periodicities are significantly different, with Polymorph B being approximately 6.1% shorter than that of Polymorph A. Furthermore, their Raman spectra, which primarily probe intra-layer vibrations, are completely dissimilar. Intriguingly, Polymorph A aligns with the crystallographically established structure, while the Raman spectrum of Polymorph B matches that widely reported in the literature. This finding resolves a long-standing discrepancy where crystallographic and spectroscopic reports have likely been examining different polymorphs unknowingly. Despite these pronounced structural differences in both inter-layer stacking and intra-layer arrangements, their optical band gaps were found to be nearly identical at ~ 3.32 eV. This work necessitates a fundamental reassessment of the GeS<sub>2</sub> material system and highlights the complex interplay between structure and electronic properties in this layered 2D material.

## Introduction

High-temperature (HT-) GeS<sub>2</sub>, a promising layered two-dimensional (2D) material, has attracted considerable attention for its potential applications in electronics and optoelectronics [1–3]. For decades, it has been widely accepted that this material crystallizes in a single, well-defined monoclinic structure with space

group P2<sub>1</sub>/c [4, 5]. Consequently, the existing spectroscopic studies [6–9], particularly Raman spectroscopy, have been conducted under the implicit assumption that they were probing this very P2<sub>1</sub>/c structure.

However, this fundamental assumption has never been critically examined. To our knowledge, no prior work has explicitly confirmed that the material used for spectroscopic analysis possesses the same

Handling Editor: Andréa de Camargo.

Address correspondence to E-mail: nakamura.masaru@nims.go.jp

crystallographic structure reported in diffraction studies. This overlooked yet critical issue forms the central motivation for our work.

In this letter, we resolve this long-standing issue by providing definitive evidence for polymorphism in HT-GeS<sub>2</sub>. We have identified two distinct polymorphs, designated Polymorph *A* and *B*. Our comprehensive analysis reveals that Polymorph *A* corresponds to the crystallographically reported phase, while Polymorph *B*, whose Raman spectrum matches previous spectroscopic studies, is a hitherto unidentified polymorph with a significantly shorter stacking periodicity. Furthermore, we report the intriguing finding that despite their pronounced structural differences, their optical band gaps are nearly identical. This work provides a new, precise framework for understanding the GeS<sub>2</sub> system and highlights the complex structure–property relationships in this layered 2D material.

## Experimental section

### Crystal growth

Single crystals of HT-GeS<sub>2</sub> were grown by the vertical Bridgman method, as described previously [10]. All characterizations were performed on as-grown, cleaved single crystals with two parallel surfaces. The preparation of a randomly oriented powder sample is extremely difficult for this material due to its pronounced preferential orientation, excellent cleavability, and ductility.

### Characterization

All structural and optical properties were characterized at room temperature.

X-ray diffraction (XRD) patterns were collected on a Rigaku SmartLabIII diffractometer with CuK $\alpha$  radiation ( $\lambda = 1.54056$  Å). To ensure the reliability of the observed peak positions, the measurements were cross-validated using a different diffractometer (Rigaku MiniFlex600).

Raman spectra were acquired using a Renishaw inVia confocal Raman microscope with a 532 nm laser excitation. The laser was focused onto the cleaved surface (the *ab*-plane) through a 5 × objective lens, and the backscattered light was collected. For polarization-dependent measurements, the spectra were recorded

before and after a 90° in-plane rotation of the crystal. The laser power on the sample was set to 10% of its maximum, which provided a sufficient signal-to-noise ratio without any observable sample degradation.

Optical transmittance spectra were recorded using a PerkinElmer Lambda 900 UV/Vis/NIR Spectrophotometer in the wavelength range of 200–2500 nm. The optical band gap ( $E_g$ ) was estimated from these spectra using the Tauc plot method.

## Results and discussion

In our routine crystal growth of HT-GeS<sub>2</sub> using the Bridgman method, we typically obtained crystals corresponding to the established P2<sub>1</sub>/c structure. We designate this standard phase as Polymorph *A*. Figure 1 compares the typical XRD patterns of the two polymorphs discussed in this study. As shown by the black line in Fig. 1, Polymorph *A*'s strongest XRD reflection consistently appears at  $2\theta = 15.5^\circ$ , a position in excellent agreement with the established crystallographic data for HT-GeS<sub>2</sub> (e.g., PDF Card No. 01–071–0366, ICSD: 1947).

Additionally, for direct comparison, the reference XRD pattern from the ICDD Powder Diffraction File (PDF Card No. 01–071–0366, ICSD: 1947) is overlaid in Fig. 1 as blue vertical bars. This reference pattern provides the expected peak positions and intensities of the established monoclinic P2<sub>1</sub>/c phase, allowing clear visual verification of the correspondence between Polymorph *A* and the standard structural data.

However, during our investigations, we made the surprising discovery that some growth runs yielded crystals with a distinctly different XRD pattern, featuring their strongest reflection at a different position,  $2\theta = 16.5^\circ$ , as shown by the red line in Fig. 1. We have designated this novel, reproducibly obtained phase as Polymorph *B*. While the precise conditions that favor the formation of Polymorph *B* are the subject of ongoing research, this paper focuses on the fundamental structural and optical characterization of these two distinct polymorphs.

The most striking difference between the two polymorphs is the position of their strongest reflection. For Polymorph *A*, this peak is located at  $2\theta = 15.5^\circ$ , whereas for Polymorph *B*, it appears at  $16.5^\circ$  (Fig. 1). This substantial difference of  $1.0^\circ$  in  $2\theta$ , observed at such a low angle region, is particularly significant and unequivocally indicates a major change in the lattice

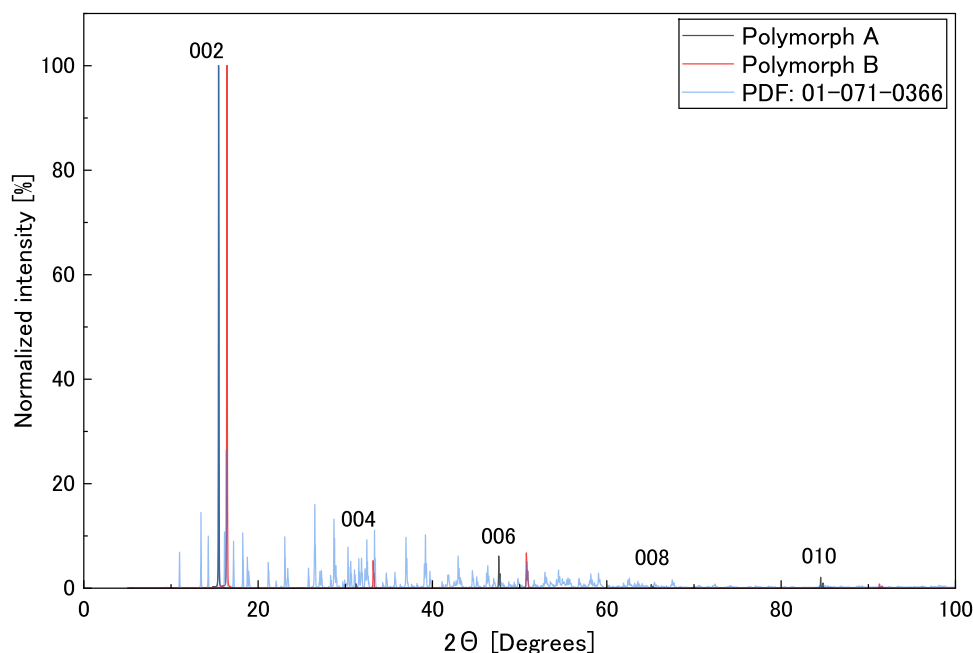


**Figure 1** XRD patterns of Polymorph A (black line) and Polymorph B (red line). The pattern for Polymorph A is indexed according to the known  $P2_1/c$  structure (PDF Card No. 01–071–0366, ICSD: 1947). For reference, the PDF pattern (blue vertical bars) is also overlaid, providing the expected peak positions for

HT-GeS<sub>2</sub>. Both patterns exhibit a series of sharp, intense peaks, confirming their highly oriented, layered nature. The fundamental lattice spacing ( $d$ ), corresponding to the stacking periodicity, is determined for each polymorph from all observed reflections, as detailed in Table 1.

spacing, far beyond any possible instrumental misalignment. To ensure the reliability of this observation, we cross-validated these peak positions using a different diffractometer (Rigaku MiniFlex600), verifying that this difference in peak position is an intrinsic property of the material and not an artifact of a single instrument.

The entire series of reflections for Polymorph A can be perfectly indexed as  $(00\ l)$  reflections ( $l = 2, 4, 6, \dots$ ). This indexing and the corresponding peak positions are in excellent agreement with the established crystallographic data from the ICDD Powder Diffraction File (PDF Card No. 01–071–0366, ICSD: 1947) for the monoclinic  $P2_1/c$  phase of HT-GeS<sub>2</sub>.

In stark contrast, the peak positions for Polymorph B, starting at  $16.5^\circ$ , do not match this established pattern, indicating a different stacking periodicity along the  $c$ -axis direction.

To quantitatively evaluate this difference, we determined the fundamental lattice spacing,  $d$ , for each polymorph from the positions of all observed peaks (Table 1). This parameter corresponds to the repeating period of the layered structure. As detailed in Table 1, the series of peaks for each polymorph can be perfectly described as higher-order reflections of a single fundamental spacing:  $d_A = 5.72 \text{ \AA}$  for Polymorph A and  $d_B = 5.39 \text{ \AA}$  for Polymorph B.

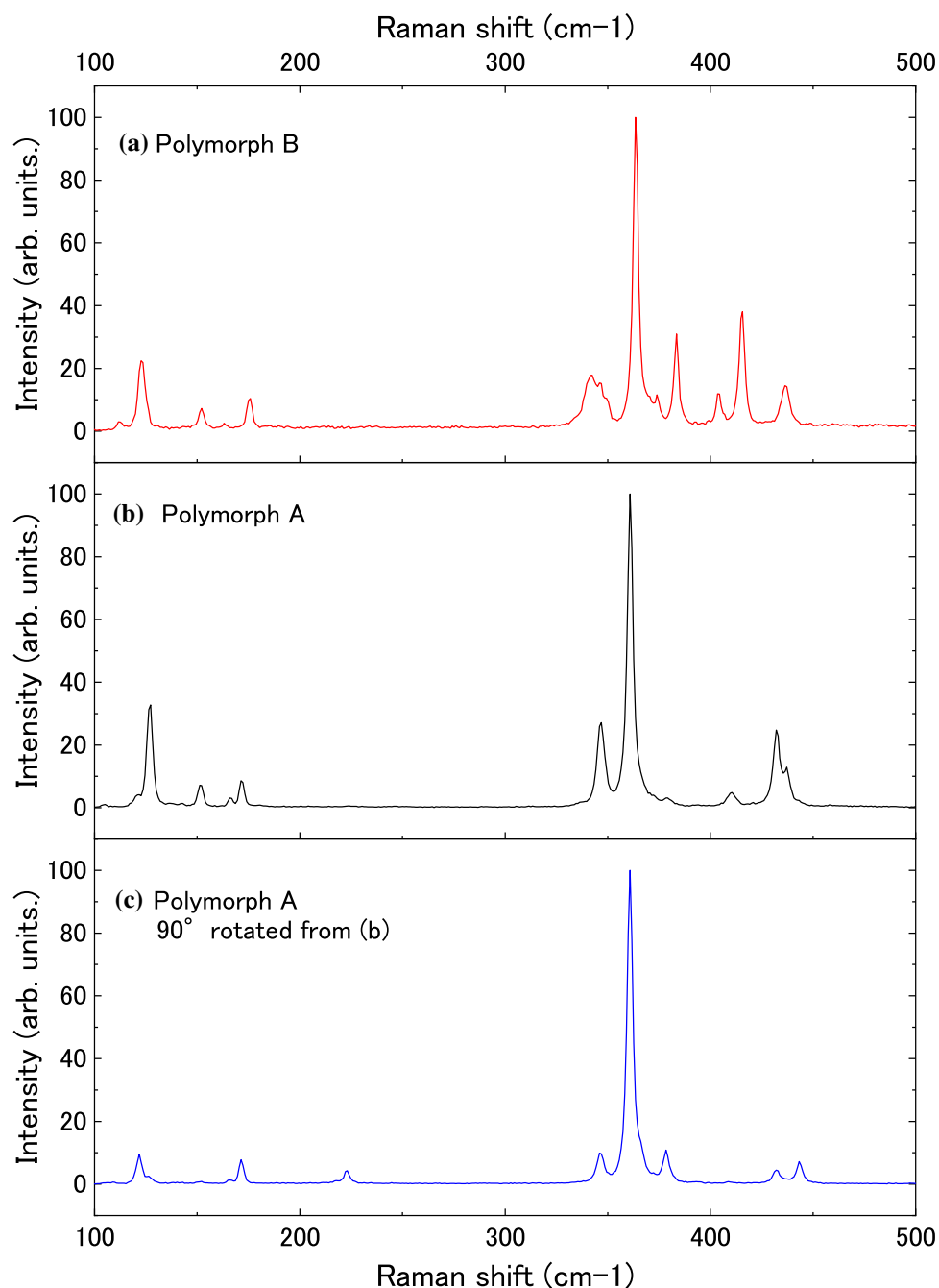
**Table 1** Observed  $2\theta$  positions for Polymorph A and B, and their corresponding lattice spacings

Polymorph A ( $15.5^\circ$ phase)		Polymorph B ( $16.5^\circ$ phase)	
Observed $2\theta$ (Degrees)	$d$ -spacing ( $\text{\AA}$ )	Observed $2\theta$ (Degrees)	$d$ -spacing ( $\text{\AA}$ )
15.48	5.72	16.44	5.39
31.32	$2.85 (\approx d/2)$	33.24	$2.69 (\approx d/2)$
47.62	$1.91 (\approx d/3)$	50.82	$1.80 (\approx d/3)$
65.46	$1.42 (\approx d/4)$	69.42	$1.35 (\approx d/4)$
84.56	$1.15 (\approx d/5)$	91.30	$1.08 (\approx d/5)$

This analysis unequivocally reveals that the fundamental spacing of Polymorph *B* is approximately 6.1% shorter than that of Polymorph *A*. This significant contraction in the stacking period unequivocally demonstrates that Polymorph *B* possesses a novel layered structure with a more compact stacking along the *c*-axis direction. To the best of our knowledge, a layered structure with this fundamental spacing has not been previously reported for the GeS<sub>2</sub> system.

The structural differences between the two polymorphs are further, and more dramatically, illuminated by their Raman spectra. Figure 2 displays the Raman spectra of both Polymorph *A* and *B*, which reveal their distinct vibrational “fingerprints.” Raman spectroscopy is a highly sensitive probe of local atomic arrangements and lattice vibrations, making it an ideal tool to distinguish between different crystalline phases.

**Figure 2** Raman spectra of the two distinct polymorphs of HT-GeS<sub>2</sub>. **a** The spectrum of Polymorph *B*, which is consistent with previous literature reports for “crystalline HT-GeS<sub>2</sub>.” **b** and **c** shows the spectra of Polymorph *A* measured at two in-plane orientations 90° apart. The dramatic difference in the spectral patterns between **a** and **b**, along with the strong polarization anisotropy observed for Polymorph *A* (cf. **b** and **c**), indicates a fundamental difference in their vibrational properties and underlying crystal structure.



In layered materials such as  $\text{GeS}_2$ , the Raman spectrum can be broadly divided into two regions. The high-frequency region (typically  $> 50 \text{ cm}^{-1}$ ) is dominated by intra-layer modes originating from the strong covalent bonds within the layers. In contrast, the low-frequency region ( $< 50 \text{ cm}^{-1}$ ) typically features weaker inter-layer modes, such as shear and layer-breathing modes, arising from the van der Waals interactions between the layers. For instance, in the case of HT- $\text{GeS}_2$ , such rigid-layer modes have been experimentally identified at 28, 32, 39, and 44/49  $\text{cm}^{-1}$  [6]. Thus, by analyzing the spectrum, we can gain insights into both the internal structure of the layers and their stacking arrangement.

Intriguingly, the spectrum of Polymorph B (Fig. 2a) is in excellent agreement with what has been widely reported in the literature as crystalline HT- $\text{GeS}_2$  [6–9]. In contrast, Polymorph A, which corresponds to the crystallographically established phase, exhibits a completely different Raman signature (Fig. 2b). Instead of the rich, multi-peak structure of Polymorph B, the spectrum of Polymorph A is strikingly simple, consisting of only a few principal peaks at entirely different positions. The clear distinction between these two spectral “fingerprints,” particularly in the number and positions of the peaks, is unequivocal evidence that they originate from different structures.

Furthermore, a significant difference in their optical anisotropy is revealed by polarization-dependent measurements. Polymorph A shows a strong polarization anisotropy, where a  $90^\circ$  in-plane rotation of the crystal leads to a dramatic change in the relative peak intensities (cf. Figure 2b and 2c). This behavior was not observed for Polymorph B, highlighting a distinct difference in the polarization response of their lattice vibrations.

It is worth noting that we also investigated the low-frequency region to search for the inter-layer vibrational modes reported by Popović and Stolz [6]. For this purpose, the spectrometer’s grating was switched from the standard 3000 l/mm to a 1000 l/mm grating to access the region close to the laser excitation line. However, even with this configuration, the weak signals expected below  $50 \text{ cm}^{-1}$  were below the detection limit of our experimental setup, likely due to the lower spectral resolution and overall sensitivity in this specific measurement condition. This finding, while being a limitation of our current measurement, does not contradict our main conclusion. Since the prominent and dramatic

spectral differences between Polymorph A and B are observed in the high-frequency region ( $> 100 \text{ cm}^{-1}$ ), it is reasonable to attribute them primarily to the disparities in their intra-layer structures. The detailed assignment of each vibrational mode is beyond the scope of this letter and remains a subject for future theoretical studies, but the stark spectral differences themselves serve as definitive proof of polymorphism in this material.

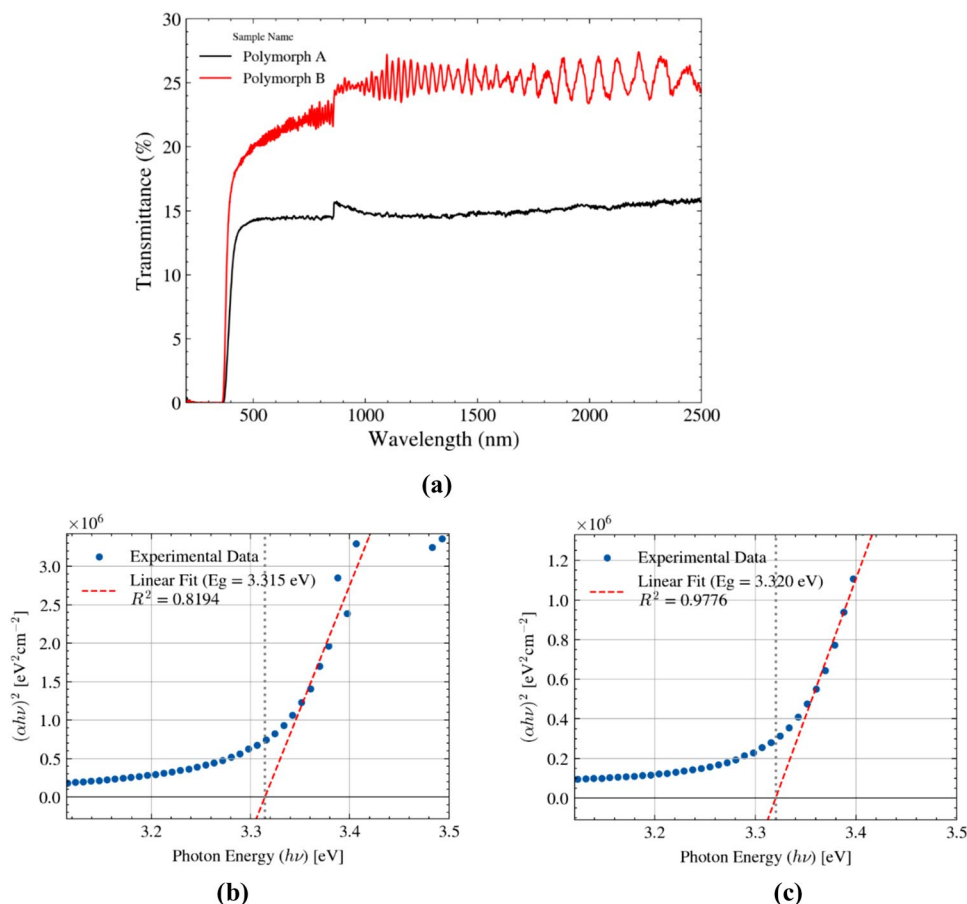
To investigate how the observed structural differences affect the electronic properties, we measured the optical transmittance of both polymorphs. The measurements were performed on samples with nearly identical thicknesses (0.181 mm for Polymorph A and 0.184 mm for Polymorph B). Figure 3a displays the resulting transmittance spectra, where the black line corresponds to Polymorph A and the red line to Polymorph B. The spectra are remarkably similar for both samples. From these transmittance data, we derived Tauc plots to estimate the optical band gap ( $E_g$ ), as presented in Figs. 3(b) and (c). In this Tauc method,  $(\alpha h\nu)^2$  is plotted against the photon energy ( $h\nu$ ), where  $\alpha$  is the absorption coefficient. For a direct band gap semiconductor, the  $E_g$  can be determined by extrapolating the linear portion of the plot to the  $(\alpha h\nu)^2 = 0$  axis.

The Tauc plot analysis led to an intriguing and unexpected finding regarding their electronic properties. As shown in Figs. 3(b) and (c), the extrapolation from the linear portion of the plots, assuming a direct band gap, yields a value of approximately  $E_g = 3.32 \text{ eV}$  for both polymorphs. Thus, despite their pronounced structural and vibrational differences, Polymorph A and Polymorph B exhibit a nearly identical optical band gap.

This remarkable result is in reasonable agreement with previously reported values for HT- $\text{GeS}_2$ , which range from 3.2 to 3.425 eV [11–13]. The most striking finding of this work, however, is not the absolute value of the band gap itself, but this unexpected invariance. It suggests that the structural modifications between Polymorph A and B, which are significant enough to alter both the inter-layer stacking periodicity and the intra-layer lattice vibrations, have a surprisingly negligible effect on the electronic transitions that define the fundamental band gap. This, in turn, implies that the electronic states at the valence band maximum and conduction band minimum are remarkably robust against these particular structural variations.



**Figure 3** Optical properties of Polymorph A and B. **a** Optical transmittance spectra of both polymorphs, where the black line corresponds to Polymorph A and the red line to Polymorph B. The measurements are performed on samples with nearly identical thicknesses (0.181 mm for A and 0.184 mm for B). **b** and **c** are the corresponding Tauc plots,  $(\alpha h\nu)^2$ , derived from the transmittance data for Polymorph A and B, respectively. The extrapolation of the linear region in each plot (dashed red line) estimates a nearly identical direct band gap of approximately 3.32 eV for both structures. The  $R^2$  values indicate the goodness of the linear fit.



## Conclusions

In summary, we have unambiguously identified two distinct polymorphs of HT-GeS<sub>2</sub>, designated as Polymorph A and B. A comprehensive characterization revealed their contrasting features:

- (i) XRD analysis demonstrated a significant difference in their inter-layer stacking periodicity.
- (ii) Raman spectroscopy highlighted fundamental disparities in their intra-layer structures.
- (iii) Surprisingly, despite these pronounced structural differences, their optical band gaps were found to be nearly identical at approximately 3.32 eV.

Our findings provide a new framework for understanding the HT-GeS<sub>2</sub> system and resolve a long-standing discrepancy in the literature, where crystallographic and spectroscopic studies may have inadvertently focused on different polymorphs. The unexpected invariance of the band gap, despite clear

structural and vibrational changes, poses a new and interesting question regarding the structure–property relationships in this layered material.

The definitive determination of the crystal structure of Polymorph B through single-crystal X-ray analysis, therefore, remains the most critical future work. Such a study will be essential to fully unravel the intricate interplay between stacking, intra-layer structure, and electronic properties in this fascinating 2D material.

## Acknowledgements

This work was supported by JSPS KAKENHI (grant number 24K08274). A part of this work was supported by “Advanced Research Infrastructure for Materials and Nanotechnology in Japan (ARIM)” of the Ministry of Education, Culture, Sports, Science and Technology (MEXT). Proposal Number JPMXP1225NM5350. The authors also thank Dr. T. Mochiku (NIMS) for helpful technical assistance with the XRD instrumentation.

## Data availability

The datasets generated and/or analyzed during the current study are included in this published article.

## Declarations

**Generative AI and AI-assisted technologies in the manuscript preparation process** During the preparation of this work the author used a large language model (LLM) from Google to refine the language and improve the overall readability of the manuscript. After using this service, the author reviewed and edited all content and takes full responsibility for the content of the published article.

**Conflict of interest** The authors declare no conflict of interest.

**Open Access** This article is licensed under a Creative Commons Attribution 4.0 International License, which permits use, sharing, adaptation, distribution and reproduction in any medium or format, as long as you give appropriate credit to the original author(s) and the source, provide a link to the Creative Commons licence, and indicate if changes were made. The images or other third party material in this article are included in the article's Creative Commons licence, unless indicated otherwise in a credit line to the material. If material is not included in the article's Creative Commons licence and your intended use is not permitted by statutory regulation or exceeds the permitted use, you will need to obtain permission directly from the copyright holder. To view a copy of this licence, visit <http://creativecommons.org/licenses/by/4.0/>.

## References

- [1] Yong JC, Hyung SI, Yoon M, Chang HK, Han SK, Seung HB, Young RL, Chan SJ, Dong MJ, Jeunghye P, Eun HC, Sung HC, Min SS, Won IC (2013) Germanium sulfide (II and IV) nanoparticles for enhanced performance of Lithium-Ion batteries. *Chem Commun* 49(41):4661–4663. <https://doi.org/10.1039/c3cc41853g>
- [2] Qifan W, Shi-Zhao K, Xiangqing L, Ying-Wei Y, Lixia Q, Jin M (2015) A facile preparation of crystalline GeS<sub>2</sub> nanoplates and their photocatalytic activity. *J Alloys Compd* 631:21–25. <https://doi.org/10.1016/j.jallcom.2014.12.259>
- [3] Jiangjing W, Ider R, Ling Z, Lu L, Volker LD, Baiyu Z, Lin T, Hongchu D, Chunlin J, Xiaofeng Q, Matthias W, Riccardo M, Wei Z (2018) Unconventional two-dimensional Germanium dichalcogenides. *Nanoscale* 10:7363. <https://doi.org/10.1039/c8nr01747f>
- [4] Rubenstein M, Roland G (1971) A monoclinic modification of Germanium disulfide, GeS<sub>2</sub>. *Acta Crystallogr B Struct Crystallogr Cryst Chem* 27(2):505–506. <https://doi.org/10.1107/S0567740871002450>
- [5] Von Dittmar G, Schäfer H (1975) Die Kristallstruktur von HT-GeS<sub>2</sub>. *Acta Crystallogr B Struct Crystallogr Cryst Chem* 31(8):2060–2064. <https://doi.org/10.1107/S0567740875006851>
- [6] Popović ZV, Stolz HJ (1981) Infrared and Raman spectra of Germanium dichalcogenides I. GeS<sub>2</sub>. *physica status solidi (b)* 106:337–348. <https://doi.org/10.1002/pssb.2221080119>
- [7] Kawamoto Y, Kawashima C (1982) Infrared and Raman spectroscopic studies on short-range structure of vitreous GeS<sub>2</sub>. *Mater Res Bull* 17:1511–1516. [https://doi.org/10.1016/0025-5408\(82\)90206-9](https://doi.org/10.1016/0025-5408(82)90206-9)
- [8] Popović ZV (1983) Molecular vibration in Sn(Pb)GeS<sub>3</sub> and GeS<sub>2</sub>. *Phys Lett A* 94:242–246. [https://doi.org/10.1016/0375-9601\(83\)90459-0](https://doi.org/10.1016/0375-9601(83)90459-0)
- [9] Inoue K, Matsuda O, Murase K (1991) Raman spectra of tetrahedral vibrations in crystalline Germanium dichalcogenides, GeS<sub>2</sub> and GeSe<sub>2</sub>, in high and low temperature forms. *Solid State Commun* 79:905–910. [https://doi.org/10.1016/0038-1098\(91\)90441-W](https://doi.org/10.1016/0038-1098(91)90441-W)
- [10] Nakamura M, Matsushita Y (2024) Optical transmittance range of high-temperature stable phase Germanium dichalcogenide (GeS<sub>2</sub>) single crystal grown by the Bridgman method. *J Cryst Growth* 647:127878. <https://doi.org/10.1016/j.jcrysgro.2024.127878>
- [11] Nikolić PM, Popović ZV (1979) Some optical properties of GeS, single crystals. *J Phys C Solid State Phys* 12:1151–1156. <https://doi.org/10.1088/0022-3719/12/6/026>
- [12] Golubkov AV, Dubrovski GB, Shelykh AI (1998) Preparation and properties of GeS<sub>2</sub> single crystals. *Semiconductors* 32:734–735
- [13] Wu CC, Ho CH, Wu JY, Lin SL, Huang YS (2005) Characterization of Ge(Se<sub>1-x</sub>S<sub>x</sub>)<sub>2</sub> series layered crystals grown by vertical Bridgman method. *J Cryst Growth* 281:377–383. <https://doi.org/10.1016/j.jcrysgro.2005.04.001>

**Publisher's Note** Springer Nature remains neutral with regard to jurisdictional claims in published maps and institutional affiliations.